

Obtaining the Current-Flux Relations of the Saturated PMSM by Signal Injection

Pascal Combes*, François Malrait*, Philippe Martin† and Pierre Rouchon†

*Schneider Toshiba Inverter Europe, 27120 Pacy-sur-Eure, France

Email: {pascal.combes, francois.malrait}@schneider-electric.com

†Centre Automatique et Systèmes, MINES ParisTech, PSL Research University, 75006 Paris, France

Email: {philippe.martin, pierre.rouchon}@mines-paristech.fr

Abstract—This paper proposes a method based on signal injection to obtain the saturated current-flux relations of a PMSM from locked-rotor experiments. With respect to the classical method based on time integration, it has the main advantage of being completely independent of the stator resistance; moreover, it is less sensitive to voltage biases due to the power inverter, as the injected signal may be fairly large.

I. INTRODUCTION

Good models are usually paramount to design good control laws. This is the case for Permanent Magnet Synchronous Motors (PMSM), especially when “sensorless” control is considered. In this mode of operation, neither the rotor position nor its velocity is measured, and the control law must make do with only current measurements; a suitable model is therefore essential to relate the currents to the other variables. When operating above moderately low speed, i.e., above about 10% of the rated speed, models neglecting magnetic saturation are usually accurate enough for control purposes; but at low speed, magnetic (cross-)saturation must be taken into account, in particular when high-frequency signal injection is used, and the more so for motors with little geometric saliency, see e.g. [1]–[6].

However, motor manufacturers very seldom provide saturation data, which means the saturated current-flux relations must be experimentally determined. The “classical” method to get these data is to integrate over time the time derivative of the flux as given by the stator model of the motor, see [7] for a detailed account. Unfortunately, this method is very sensitive to the value of the stator resistance R_s , which may significantly vary during a long experiment; it also requires a good knowledge of the actually impressed potentials (voltage sensors may be required because of the not very well-known voltage drops in the power stage), and of course of the resulting currents (which are in practice always measured). It is thus not easy to implement this method on a commercial variable speed drive for use in the field.

The goal of this paper is to propose an alternative approach to obtain the saturated current-flux relations, which is completely independent on the knowledge of the stator resistance R_s ; it is also less sensitive to the voltage

drops of the power stage. It is based on high-frequency signal injection. It is based on signal injection, a technique that was originally introduced for sensorless control at low velocity [8], but that can also be used for identification [9]. The key idea, thanks to a suitable analysis of the effects of signal injection, is to recover the flux-current relations by integrating over paths in the plane of direct and quadrature currents; it generalizes a cruder procedure used in [10]. Notice that the required experimental data can be obtained with only experiments where the rotor is locked in a known position, which is reasonable for industrial use in the field (the classical method also works in similar conditions).

The paper runs as follows: section II presents the structure of the model, based on an energy approach; section III applies the classical method to a test PMSM; section IV details the proposed approach, and applies it to the same test PMSM.

The following conventions are used: if x^{ij} , ij being $\alpha\beta$ or DQ , is the vector with coordinates x^i and x^j , we write indifferently x^{ij} and $(x^i, x^j)^T$; if f is a function of several variables, $\partial_k f$ denotes its partial derivative with respect to the k^{th} variable, and $\partial_{kl}^2 f = \partial_{lk}^2 f$ the second partial derivative with respect to the k^{th} and l^{th} variables. Lastly, the rotation matrix of angle α is denoted by $\mathcal{R}(\alpha) := \begin{pmatrix} \cos \alpha & -\sin \alpha \\ \sin \alpha & \cos \alpha \end{pmatrix}$; of course, $\mathcal{R}(\alpha)\mathcal{R}^T(\alpha) = \begin{pmatrix} 1 & 0 \\ 0 & 1 \end{pmatrix}$, where $\mathcal{R}^T(\alpha)$ is the transpose of $\mathcal{R}(\alpha)$.

II. ENERGY-BASED MODEL OF THE PMSM

To write a model of the star-connected saturated sinusoidal PMSM in the DQ frame, we follow the energy-based approach of [11], [12]. All the motor specific information is encoded in the scalar magnetic energy function $\mathcal{H}_m^{DQ}(\phi_s^{DQ})$, where ϕ_s^{DQ} is the flux linkage vector. \mathcal{H}_m^{DQ} is independent of the (electrical) rotor angle θ by the assumption of sinusoidal windings, and independent of the (electrical) rotor velocity ω as in any conventional electromechanical device. The state equations of the PMSM then read

$$\frac{d\phi_s^{DQ}}{dt} = v_s^{DQ} - R_s i_s^{DQ} - \omega \mathcal{J} \phi_s^{DQ} \quad (1)$$

$$\frac{J_l}{n} \frac{d\omega}{dt} = -n \phi_s^{DQ T} \mathcal{J} i_s^{DQ} - T_l \quad (2)$$

$$\frac{d\theta}{dt} = \omega, \quad (3)$$

where v_s^{DQ} is the impressed potential vector, R_s the stator resistance, n the number of pole pairs, T_l the load torque and $\mathcal{J} := \begin{pmatrix} 0 & -1 \\ 1 & 0 \end{pmatrix}$; the stator current vector i_s^{DQ} is the gradient of \mathcal{H}_m^{DQ} , i.e.,

$$i_s^{DQ} := \nabla \mathcal{H}_m^{DQ}(\phi_s^{DQ}) = \begin{pmatrix} \partial_1 \mathcal{H}_m^{DQ}(\phi_s^D, \phi_s^Q) \\ \partial_2 \mathcal{H}_m^{DQ}(\phi_s^D, \phi_s^Q) \end{pmatrix}. \quad (4)$$

The physical control input is the potential vector $v_s^{\alpha\beta} := \mathcal{R}(\theta)v_s^{DQ}$ impressed in the $\alpha\beta$ frame, i.e., the (fictitious) potential vector v_s^{DQ} rotated by $\mathcal{R}(\theta)$. Similarly, the measured current vector is $i_s^{\alpha\beta} := \mathcal{R}(\theta)i_s^{DQ}$; in sensorless control, this is the only available measurement.

Taking advantage of the construction symmetries of the PMSM (the stator and the rotor of the PMSM are symmetric with respect to a plane), see [12] for details, we can moreover write

$$\mathcal{H}_m^{DQ}(\phi_s^D, -\phi_s^Q) = \mathcal{H}_m^{DQ}(\phi_s^D, \phi_s^Q), \quad (5)$$

i.e., the magnetic energy function \mathcal{H}_m^{DQ} of a PMSM is even with respect to the q -axis flux linkage ϕ_s^Q .

Notice that thanks to the assumption of sinusoidal windings, all that is needed to close the model (1)–(3) are the flux-current relations (4); this is no longer the case for non-sinusoidal windings, since the electro-magnetic torque in (3) explicitly depends on \mathcal{H}_m^{DQ} . Notice also that the simplest acceptable function is the quadratic form

$$\mathcal{H}_m^{DQ}(\phi_s^{DQ}) := \frac{1}{2L^D}(\phi_s^D - \Phi_M)^2 + \frac{1}{2L^Q}\phi_s^{Q2},$$

which yields the current-flux relations

$$i_s^D = \frac{\phi_s^D - \Phi_M}{L^D}$$

$$i_s^Q = \frac{\phi_s^Q}{L^Q}$$

and the electro-magnetic torque

$$T_e = \frac{n}{L^D}\Phi_M\phi_s^Q + n\left(\frac{1}{L^Q} - \frac{1}{L^D}\right)\phi_s^D\phi_s^Q;$$

in other words, the simplest acceptable magnetic energy function represents the unsaturated PMSM. The unsaturated model is usually sufficient for control above moderately low speed.

This energy approach enjoys several interesting features:

- it naturally enforces the reciprocity conditions $\frac{\partial i_s^D}{\partial \phi_s^Q} = \frac{\partial i_s^Q}{\partial \phi_s^D}$ [13], since $\partial_{12}^2 \mathcal{H}_m^{DQ}(\phi_s^D, \phi_s^Q) = \partial_{21}^2 \mathcal{H}_m^{DQ}(\phi_s^D, \phi_s^Q)$
- it yields a valid expression for the magnetic torque, even in the presence of magnetic saturation
- it justifies the modeling of saturation in the fictitious rotor DQ frame for a star-connected motor. Though this point is usually taken for granted, it is not completely obvious because of the nonlinearities due to saturation that: i) the transformation from

the physical abc -frame to the fictitious $DQ0$ -frame behaves well; ii) the decoupling between the DQ - and the 0-axes is still valid

- it requires only a very basic knowledge of the motor internal layout
- finally, it is particularly amenable to an analysis of the effects of signal injection.

In all the experiments, the rotor will be locked in a known position, so that (1)–(3) reduces to

$$\frac{d\phi_s^{DQ}}{dt} = \mathcal{R}^T(\theta_{lr})v_s^{\alpha\beta} - R_s i_s^{DQ}, \quad (6)$$

with θ_{lr} constant and known. Notice that since θ_{lr} is known, we can consider that $v_s^{DQ} := \mathcal{R}^T(\theta_{lr})v_s^{\alpha\beta}$ is the impressed potential, and $i_s^{DQ} := \mathcal{R}^T(\theta_{lr})i_s^{\alpha\beta}$ is the available measurement.

III. CLASSICAL METHOD

The most widely used method to obtain the current-flux relations, see [7], assumes that an impressed potential trajectory $t \mapsto v_s^{DQ}(t)$ is known, together with the resulting current trajectory $t \mapsto i_s^{DQ}(t)$. The corresponding flux linkage is obtained by time integrating (6), i.e.,

$$\phi_s^{DQ}(t) = \phi_s^{DQ}(0) + \int_0^t (v_s^{DQ}(\tau) - R_s i_s^{DQ}(\tau)) d\tau, \quad (7)$$

the unknown initial value $\phi_s^{DQ}(0)$ being yet to determine. A pair $(i_s^{DQ}(t), \phi_s^{DQ}(t))$ is thus obtained for each time t ; provided the current trajectory $t \mapsto i_s^{DQ}(t)$ covers a sufficient area of the current plane, this yields the desired current-flux relations. The initial value $\phi_s^{DQ}(0)$ is chosen so as the flux linkage is zero when the current is zero.

Thanks to the filtering effect of the integration, the method is rather insensitive to measurement noise. However, it is strongly affected by biases in:

- the impressed potential. The power stage is usually an IGBT bridge commuted with PWM; owing to voltage drops in the transistors and dead times, the actually impressed potential somewhat differs from the desired one, see e.g. [14]. This is not a problem if voltage sensors are available, as in a laboratory experiment, but matters for implementation on industrial drives, which are usually not equipped with such sensors
- the stator resistance R_s estimation; this is the main problem, since the value of the resistance can significantly vary during a long experiment.

A. Experimental results

The method was used to obtain the current-flux curves of a 400 W PMSM (rated parameters in table I). The motor is fed by an 1.5 kW ATV71 (ATV71HU15N4) inverter bridge driven by a dSpace board (DS1005). The rotor was first aligned so that the $\alpha\beta$ and DQ frames coincide, and then locked with a mechanical brake. To check the consistency of the results, three trajectories were used:

Table I
RATED PARAMETERS OF TEST PMSM.

Rated power	400 W
Rated voltage (RMS)	139.3 V
Rated current (RMS)	1.66 A
Rated frequency	60 Hz
Rated speed	1800 rpm
Rated torque	2.12 N m
Number of pole pairs n	2
Stator resistance R_s	4.25 Ω
D -axis inductance L^D	43.25 mH
Q -axis inductance L^Q	69.05 mH

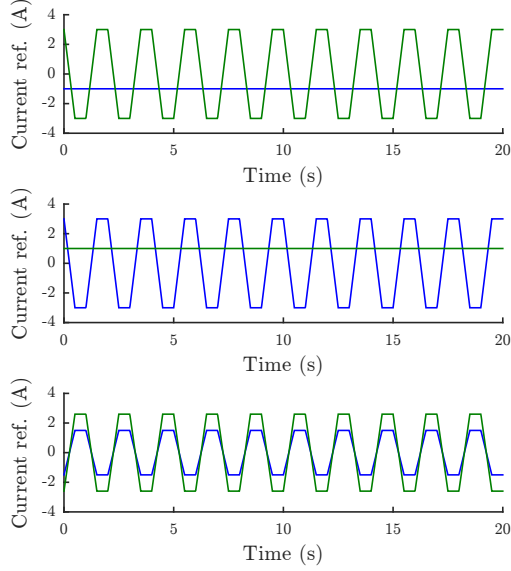


Figure 1. The three current trajectories on D - (—) and Q -axis (---) used in the experiment.

- constant i_s^D , 2s-periodic trapezoidal i_s^Q with amplitude 3 A, see fig. 1(top); the experiment was repeated for $i_s^D := -3\text{ A}, -2\text{ A}, -1\text{ A}, 0\text{ A}, 1\text{ A}, 2\text{ A}$ and 3 A
- constant i_s^Q , 2s-periodic trapezoidal i_s^D with amplitude 3 A, see fig. 1(middle); the experiment was repeated for $i_s^Q := -3\text{ A}, -2\text{ A}, -1\text{ A}, 0\text{ A}, 1\text{ A}, 2\text{ A}$ and 3 A
- proportional 2s-periodic trapezoidal currents on both axes with total amplitude 3 A, see fig. 1(bottom).

To enforce these trajectories, the currents were controlled with Proportional-Integral controllers on the D - and Q -axes (damping ratio $\xi := \frac{1}{\sqrt{2}}$; bandwidth $\omega_0 := 25\text{ Hz}$).

The stator resistance is evaluated by computing the ratio between the voltage and the current during the phases when the current is constant; it is found to vary from 4.5 A to 5.25 A over the whole experiment.

The flux linkage is then computed according to (7). The sensitivity to voltage biases is illustrated in fig. 2: when the time integration is performed over several identical similar patterns (10 in our case), the shape of the experimental

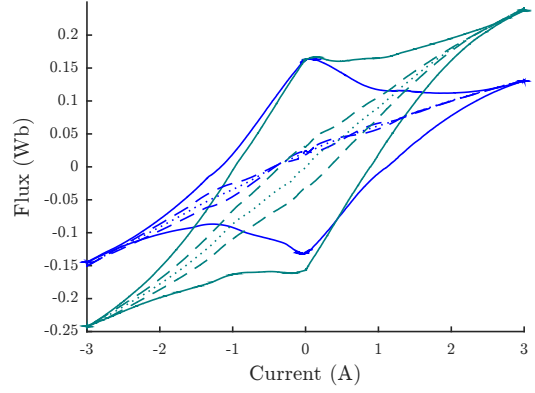


Figure 2. Experimental current-flux curves $\phi_s^D(i_s^D, 0) - \Phi_M$ (—) and $\phi_s^Q(0, i_s^Q)$ (---); solid lines: uncompensated voltage drops; dashed lines: compensated voltage drops; dotted line: averaged curve.

current-flux curve is altered, especially when the current is small; with uncompensated inverter voltage drops and dead times, the result is very bad (solid lines); with compensation by a suitable model, the loop in the current-flux curve is much smaller, but still present (dashed lines); the final current-flux curve is then obtained by averaging all the flux linkages points obtained for a current point (dotted line).

The full 3D current-flux relations are displayed in fig. 3. The magnetic saturation is clearly visible. As expected from (5), which implies

$$\begin{aligned}\partial_1 \mathcal{H}_m^{DQ}(\phi_s^D, -\phi_s^Q) &= \partial_1 \mathcal{H}_m^{DQ}(\phi_s^D, \phi_s^Q) \\ \partial_2 \mathcal{H}_m^{DQ}(\phi_s^D, -\phi_s^Q) &= -\partial_1 \mathcal{H}_m^{DQ}(\phi_s^D, \phi_s^Q),\end{aligned}$$

it can be seen that ϕ_s^D is even with respect to i_s^Q , and ϕ_s^Q odd with respect to i_s^Q .

IV. PROPOSED METHOD

A. Data acquisition with signal injection

Signal injection was originally introduced for sensorless control at low velocity [8], but it can also be used for identification [9]. We follow the quantitative analysis introduced in [6], [9] and studied in detail in [15]; it is valid even in the presence of nonlinearities due to magnetic saturation, and whatever the shape of the (periodic) injected signal. Impressing in (6) a potential vector of the form

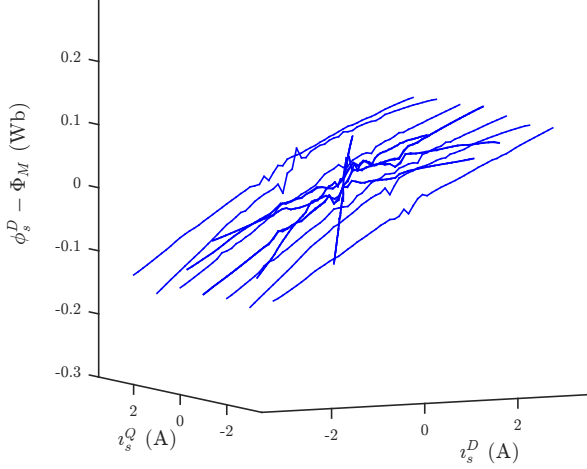
$$v_s^{\alpha\beta} = \overline{v_s^{\alpha\beta}} + \widetilde{v_s^{\alpha\beta}} f(\Omega t), \quad (8)$$

where f a 1-periodic function and Ω is a “large” frequency, the analysis shows that the actual flux linkage is

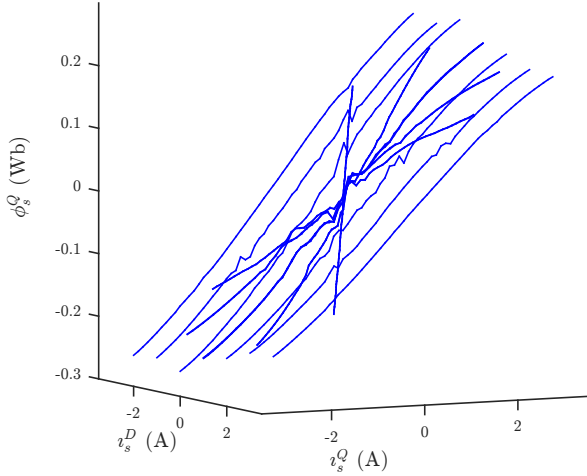
$$\phi_s^{DQ} = \overline{\phi_s^{DQ}} + \frac{1}{\Omega} \mathcal{R}^T(\theta_{lr}) \widetilde{v_s^{\alpha\beta}} F(\Omega t) + \mathcal{O}\left(\frac{1}{\Omega^2}\right), \quad (9)$$

where F is the primitive of f with zero mean, and \mathcal{O} is the “big-O” symbol of analysis; $\overline{\phi_s^{DQ}}$ is the flux linkage without signal injection, i.e., the solution of

$$\frac{d\overline{\phi_s^{DQ}}}{dt} = \mathcal{R}^T(\theta_{lr}) \overline{v_s^{\alpha\beta}} - R_s \overline{i_s^{DQ}}.$$



(a) D -axis flux linkage in function of i_s^{DQ}



(b) Q -axis flux linkage in function of i_s^{DQ}

Figure 3. Current-flux relations obtained by the classical method.

Plugging (9) into (4) and expanding then yields

$$i_s^{\alpha\beta} = \overline{i_s^{\alpha\beta}} + \frac{1}{\Omega} \widetilde{\gamma^{\alpha\beta}} F(\Omega t) + \mathcal{O}\left(\frac{1}{\Omega^2}\right), \quad (10)$$

where $\widetilde{\gamma^{\alpha\beta}} := \mathcal{S}(\theta_{lr}, \overline{\phi_s^{DQ}}) \overline{v_s^{\alpha\beta}}$ and

$$\mathcal{S}(\theta, \phi) := \mathcal{R}(\theta) \begin{pmatrix} \partial_{11}^2 \mathcal{H}_m^{DQ}(\phi) & \partial_{12}^2 \mathcal{H}_m^{DQ}(\phi) \\ \partial_{12}^2 \mathcal{H}_m^{DQ}(\phi) & \partial_{22}^2 \mathcal{H}_m^{DQ}(\phi) \end{pmatrix} \mathcal{R}^T(\theta).$$

We call $\mathcal{S}(\theta_{lr}, \overline{\phi_s^{DQ}})$ the “saliency matrix”; indeed, it effectively depends on θ_{lr} if the motor exhibits saliency, whether geometric or induced by magnetic saturation. In other words, (10) shows that a small ripple of amplitude $\widetilde{i_s^{\alpha\beta}} := \frac{1}{\Omega} \widetilde{\gamma^{\alpha\beta}}$, produced by the injected signal $\overline{v_s^{\alpha\beta}} f(\Omega t)$, is superimposed to the current without signal injection $\overline{i_s^{\alpha\beta}}$, produced by $\overline{v_s^{\alpha\beta}}$. As explained in [15], both $\overline{i_s^{\alpha\beta}}$ and $\widetilde{i_s^{\alpha\beta}}$

can be extracted from the actual measurement $i_s^{\alpha\beta}$ using the estimations

$$\begin{aligned} \overline{i_s^{\alpha\beta}}(t) &= \Omega \int_{t-\frac{1}{\Omega}}^t i_s^{\alpha\beta}(\tau) d\tau \\ \widetilde{i_s^{\alpha\beta}}(t) &= \Omega \frac{\int_{t-\frac{1}{\Omega}}^t \left(i_s^{\alpha\beta}(\tau - \frac{1}{2\Omega}) - \overline{i_s^{\alpha\beta}}(\tau) \right) F(\Omega\tau) d\tau}{\int_{t-\frac{1}{\Omega}}^t F^2(\Omega t) dt}. \end{aligned}$$

In other words, the “virtual” measurement $\widetilde{i_s^{\alpha\beta}}$ has been made available besides the “actual” measurement $\overline{i_s^{\alpha\beta}}$.

Notice that since θ_{lr} is known, we can consider that $\overline{v_s^{DQ}} := \mathcal{R}^T(\theta_{lr}) v_s^{\alpha\beta}$ and $v_s^{DQ} := \mathcal{R}^T(\theta_{lr}) \overline{v_s^{\alpha\beta}}$ are the impressed potentials, and that $\overline{i_s^{DQ}} := \mathcal{R}^T(\theta_{lr}) \overline{i_s^{\alpha\beta}}$ and $i_s^{DQ} := \mathcal{R}^T(\theta_{lr}) \widetilde{i_s^{\alpha\beta}}$, are the available measurements. It is then possible to experimentally acquire the six expressions

Experimentally, it is possible to apply any desired current $\overline{i_s^{DQ}}$ by a suitable choice of $\overline{v_s^{DQ}}$; by signal injection with at least two independent vectors $\overline{v_s^{DQ}}$ and extraction of the corresponding $\overline{i_s^{DQ}}$, it is then possible to obtain the complete saliency matrix, hence $\partial_{11}^2 \mathcal{H}_m^{DQ}(\overline{\phi_s^{DQ}})$, $\partial_{22}^2 \mathcal{H}_m^{DQ}(\overline{\phi_s^{DQ}})$ and $\partial_{12}^2 \mathcal{H}_m^{DQ}(\overline{\phi_s^{DQ}})$.

Since the flux linkage $\overline{\phi_s^{DQ}}$ is unknown, what is actually obtained is $H_{11}(\overline{i_s^{DQ}})$, $H_{12}(\overline{i_s^{DQ}})$ and $H_{22}(\overline{i_s^{DQ}})$, where $H_{kl}(\overline{i_s^{DQ}}) := \partial_{kl}^2 \mathcal{H}_m^{DQ}(\overline{\Phi_s^{DQ}}(\overline{i_s^{DQ}}))$ and $\overline{\Phi_s^{DQ}}$ is the inverse of the flux-current relation (4).

B. Obtaining the current-flux relations from the $H_{kl}(\overline{i_s^{DQ}})$

By the very definition of $\overline{\Phi_s^{DQ}}$, we can write $\overline{i_s^{DQ}} = \nabla \mathcal{H}_m^{DQ}(\overline{\Phi_s^{DQ}}(\overline{i_s^{DQ}}))$, or, more explicitly,

$$\begin{aligned} \overline{i_s^D} &= \partial_1 \mathcal{H}_m^{DQ}(\overline{\Phi_s^D}(\overline{i_s^D}, \overline{i_s^Q}), \overline{\Phi_s^Q}(\overline{i_s^D}, \overline{i_s^Q})) \\ \overline{i_s^Q} &= \partial_2 \mathcal{H}_m^{DQ}(\overline{\Phi_s^D}(\overline{i_s^D}, \overline{i_s^Q}), \overline{\Phi_s^Q}(\overline{i_s^D}, \overline{i_s^Q})). \end{aligned}$$

Differentiating these relations with respect to $\overline{i_s^D}$ and $\overline{i_s^Q}$, we find that

$$\begin{pmatrix} H_{11}(\overline{i_s^{DQ}}) & H_{12}(\overline{i_s^{DQ}}) \\ H_{12}(\overline{i_s^{DQ}}) & H_{22}(\overline{i_s^{DQ}}) \end{pmatrix} \begin{pmatrix} \partial_1 \overline{\Phi_s^D}(\overline{i_s^{DQ}}) & \partial_2 \overline{\Phi_s^D}(\overline{i_s^{DQ}}) \\ \partial_1 \overline{\Phi_s^Q}(\overline{i_s^{DQ}}) & \partial_2 \overline{\Phi_s^Q}(\overline{i_s^{DQ}}) \end{pmatrix}$$

is the identity matrix, which implies

$$\begin{aligned} \begin{pmatrix} \partial_1 \overline{\Phi_s^D}(\overline{i_s^{DQ}}) & \partial_2 \overline{\Phi_s^D}(\overline{i_s^{DQ}}) \\ \partial_1 \overline{\Phi_s^Q}(\overline{i_s^{DQ}}) & \partial_2 \overline{\Phi_s^Q}(\overline{i_s^{DQ}}) \end{pmatrix} &= \begin{pmatrix} H_{kl}(\overline{i_s^{DQ}}) & H_{kl}(\overline{i_s^{DQ}}) \\ H_{kl}(\overline{i_s^{DQ}}) & H_{kl}(\overline{i_s^{DQ}}) \end{pmatrix}^{-1} \\ &=: \begin{pmatrix} L_{dd}(\overline{i_s^{DQ}}) & L_{dq}(\overline{i_s^{DQ}}) \\ L_{dq}(\overline{i_s^{DQ}}) & L_{qq}(\overline{i_s^{DQ}}) \end{pmatrix}. \end{aligned}$$

We thus know the partial derivatives of $\overline{\Phi_s^{DQ}}$, or, equivalently, the integrable differential forms

$$\begin{aligned} d\overline{\Phi_s^D}(\overline{i_s^{DQ}}) &= L_{dd}(\overline{i_s^{DQ}}) d\overline{i_s^D} + L_{dq}(\overline{i_s^{DQ}}) d\overline{i_s^Q} \\ d\overline{\Phi_s^Q}(\overline{i_s^{DQ}}) &= L_{dq}(\overline{i_s^{DQ}}) d\overline{i_s^D} + L_{qq}(\overline{i_s^{DQ}}) d\overline{i_s^Q}. \end{aligned}$$

To recover Φ_s^{DQ} , we integrate these forms on paths $\kappa \mapsto i_s^{DQ} = I_s^{DQ}(\kappa)$ in the current plane. This yields

$$\begin{aligned} \Phi_s^D(I_s^{DQ}(\kappa)) - \Phi_s^D(I_s^{DQ}(\kappa_0)) &= \int_{\kappa_0}^{\kappa} \frac{d\Phi_s^D}{d\zeta}(I_s^{DQ}(\zeta))d\zeta \\ &= \int_{\kappa_0}^{\kappa} L_{dd}(I_s^{DQ}(\zeta)) \frac{dI_s^D}{d\zeta}(\zeta)d\zeta \\ &\quad + \int_{\kappa_0}^{\kappa} L_{dq}(I_s^{DQ}(\zeta)) \frac{dI_s^Q}{d\zeta}(\zeta)d\zeta, \end{aligned} \quad (11)$$

and a similar expression for $\Phi_s^Q(I_s^{DQ}(\kappa))$. Therefore, for each κ , a couple $(I_s^{DQ}(\kappa), \Phi_s^D(I_s^{DQ}(\kappa)))$ is obtained; provided the current paths $\kappa \mapsto I_s^{DQ}(\kappa)$ cover a sufficient area of the current plane, this yields the desired current-flux relations. The initial value $\Phi_s^{DQ}(I_s^{DQ}(\kappa_a))$ is chosen so as the flux linkage is zero when the current is zero.

Notice the method is completely immune to errors in the knowledge of the stator resistance R_s , since it never explicitly uses its value. Moreover, it is less sensitive than the classical method to imperfections of the power inverter because the base potential v_s^{DQ} does not need to be known, whereas the injected potential v_s^{DQ} can be fairly large.

C. Experimental results

The proposed approach was applied with the same experimental conditions as in section III-A, with similar desired currents paths. Nevertheless, the currents were not enforced by controllers not to disturb the signal injection. As a consequence the actual currents paths slightly differ from the desired ones, see fig. 4; this is not a problem since the true values of i_s^{DQ} are known. The current paths were discretized with steps Δi_s^{DQ} of about 0.1 A; for each current point i_s^{DQ} , the injected signal was a 5 s long square signal of frequency $\Omega := 500$ Hz and amplitude $\tilde{u}_s := 40$ V, slowly rotating at frequency $f_i := 1$ Hz,

$$\tilde{u}_s^{DQ} := \tilde{u}_s \begin{pmatrix} \cos(2\pi f_i t) \\ \sin(2\pi f_i t) \end{pmatrix}.$$

The corresponding current ripple, namely

$$\tilde{i}_s^{DQ} = \frac{\tilde{u}_s}{\Omega} \begin{pmatrix} H_{11}(\tilde{i}_s^{DQ}) \cos(2\pi f_i t) + H_{12}(\tilde{i}_s^{DQ}) \sin(2\pi f_i t) \\ H_{12}(\tilde{i}_s^{DQ}) \cos(2\pi f_i t) + H_{22}(\tilde{i}_s^{DQ}) \sin(2\pi f_i t) \end{pmatrix},$$

then directly yields $H_{11}(\tilde{i}_s^{DQ})$, $H_{12}(\tilde{i}_s^{DQ})$ and $H_{22}(\tilde{i}_s^{DQ})$. The interest of slowly rotating the injected signal is to provide many measurements points i_s^{DQ} , hence an accurate determination of $H_{11}(\tilde{i}_s^{DQ})$, $H_{12}(\tilde{i}_s^{DQ})$ and $H_{22}(\tilde{i}_s^{DQ})$.

The flux linkage along a current path is then obtained by discretizing the integrals in (11),

$$\begin{aligned} \Phi_s^D(I_s^{DQ}(\kappa)) - \Phi_s^D(I_s^{DQ}(\kappa_0)) \\ \approx \sum_{\zeta=\kappa_0+1}^{\kappa} L_{dd}(I_s^{DQ}(\zeta))\Delta I_s^D(\zeta) + L_{dq}(I_s^{DQ}(\zeta))\Delta I_s^Q(\zeta), \end{aligned}$$

where $\Delta I_s^{DQ}(\zeta) := I_s^{DQ}(\zeta) - I_s^{DQ}(\zeta - 1)$. The current-flux curves so obtained are displayed in fig. 5. The consistency

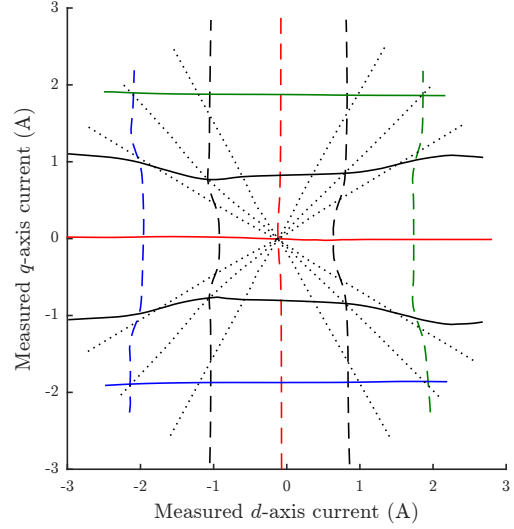


Figure 4. Actual i_s^{DQ} paths.

can be checked by computing the flux linkage difference at points where the current paths intersect, which should be zero in theory: the maximum relative error is 1.3% for the D -axis flux and 2.9% for the Q -axis. Moreover, as with the classical method, ϕ_s^D is even with respect to i_s^Q , and ϕ_s^Q odd with respect to i_s^Q .

Notice the method provides the Hessian matrix of the energy function

$$\begin{pmatrix} \partial_{11}^2 \mathcal{H}_m^{DQ} & \partial_{11}^2 \mathcal{H}_m^{DQ} \\ \partial_{11}^2 \mathcal{H}_m^{DQ} & \partial_{11}^2 \mathcal{H}_m^{DQ} \end{pmatrix},$$

in function of i_s^{DQ} or ϕ_s^{DQ} , i.e., the partial derivatives of the current-flux relations. It is a useful piece of information for fitting a parametric model to the current-flux relations; indeed, it is numerically better to fit the derivatives of a function than the function itself. It also provides its inverse matrix,

$$\begin{pmatrix} L_{dd} & L_{dq} \\ L_{dq} & L_{qq} \end{pmatrix},$$

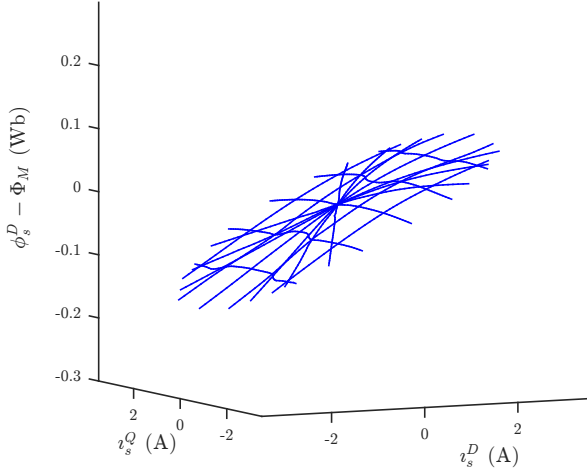
which is the inductance matrix. As expected from (5), which implies

$$\begin{aligned} \partial_{11}^2 \mathcal{H}_m^{DQ}(\phi_s^D, -\phi_s^Q) &= \partial_{11}^2 \mathcal{H}_m^{DQ}(\phi_s^D, \phi_s^Q) \\ \partial_{22}^2 \mathcal{H}_m^{DQ}(\phi_s^D, -\phi_s^Q) &= \partial_{22}^2 \mathcal{H}_m^{DQ}(\phi_s^D, \phi_s^Q) \\ \partial_{12}^2 \mathcal{H}_m^{DQ}(\phi_s^D, -\phi_s^Q) &= -\partial_{12}^2 \mathcal{H}_m^{DQ}(\phi_s^D, \phi_s^Q), \end{aligned}$$

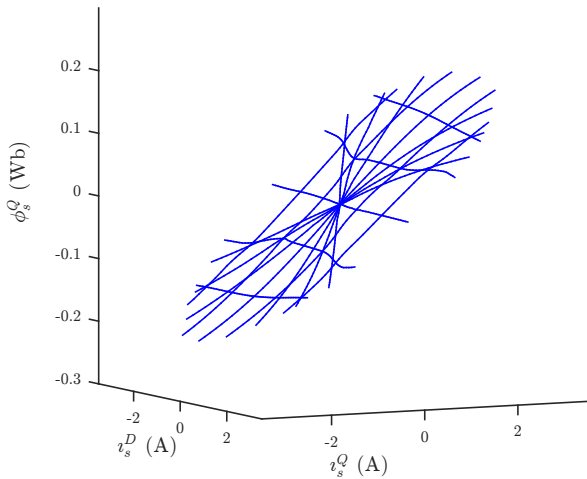
the parity/impairity relations are experimentally satisfied, both for the Hessian matrix and its inverse. This is illustrated for the inductance matrix in in fig. 6; the (cross)-saturation is even more visible than in fig. 5.

D. Comparison with the classical method

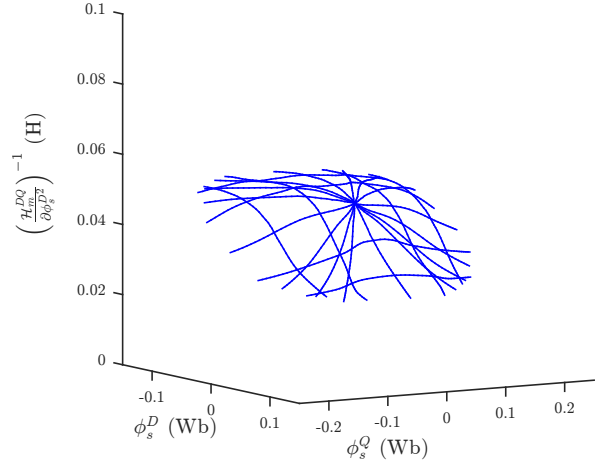
Fig. 7 compares some current-flux curves obtained by the classical and the proposed method. The two methods yield similar curves, with nevertheless some small



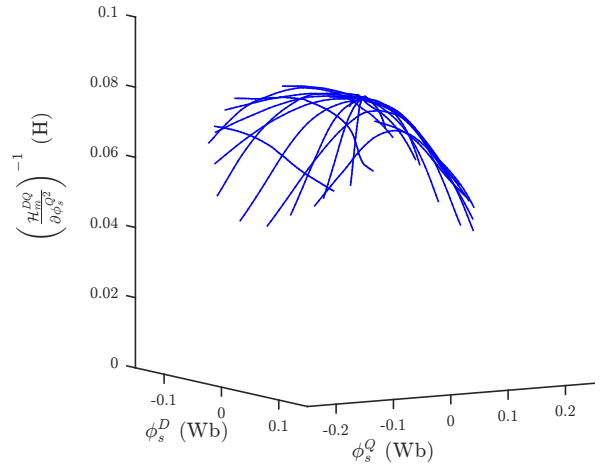
(a) D-axis flux linkage in function of i_s^{DQ}



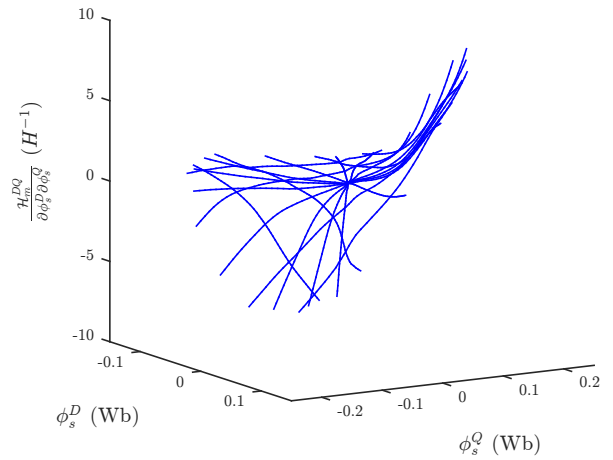
(b) Q-axis flux linkage in function of i_s^{DQ}



(a) L_{dd} as a function of ϕ_s^{DQ}



(b) L_{qq} as a function of ϕ_s^{DQ}



(c) L_{qq} as a function of ϕ_s^{DQ}

Figure 5. Current-flux relations obtained by the proposed method.

differences. Some of the differences could be explained by experimental errors, especially biases in the classical method. Another possibility is that, owing to hysteresis, the flux linkage computed by signal injection is systematically smaller than the flux linkage computed by the classical method; this was noticed for the Synchronous Reluctance Motor in [10], and raises the question of which model should be used for sensorless control at low velocity.

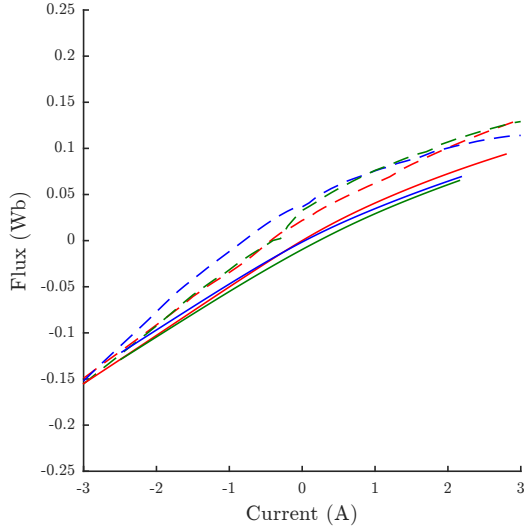
V. CONCLUSION

We have proposed a method based on signal injection to obtain the saturated current-flux relations of a PMSM from locked-rotor experiments. With respect to the classical method based on time integration, it has the main advantage of being completely independent of the stator resistance; moreover, it is less sensitive to voltage biases

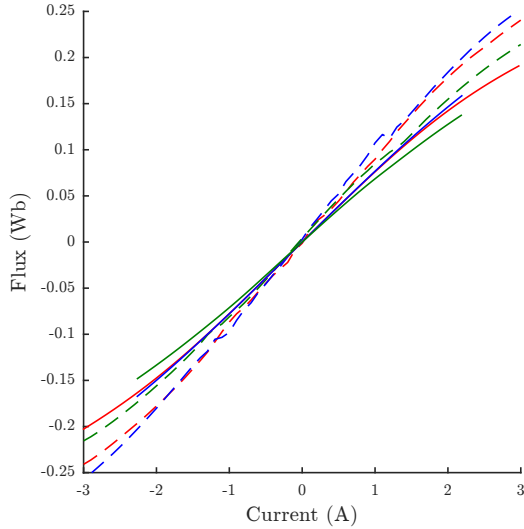
Figure 6. Coefficients of inductance matrix obtained by the proposed method.

REFERENCES

- [1] D. D. Reigosa, P. Garcia, D. Raca, F. Briz, and R. D. Lorenz, "Measurement and adaptive decoupling of cross-saturation effects and secondary saliencies in sensorless controlled IPM synchronous machines," *IEEE Transactions on Industry Applications*, vol. 44, no. 6, pp. 1758–1767, Nov. 2008.
- [2] Y. Li, Z. Zhu, D. Howe, C. Bingham, and D. Stone, "Improved rotor-position estimation by signal injection in brushless AC motors, accounting for cross-coupling magnetic saturation," *IEEE Transactions on Industry Applications*, vol. 45, pp. 1843–1850, 2009.
- [3] P. Sergeant, F. De Belie, and J. Melkebeek, "Effect of rotor geometry and magnetic saturation in sensorless control of PM synchronous machines," *IEEE Trans. Magnetics*, vol. 45, no. 3, pp. 1756–1759, 2009.
- [4] N. Bianchi, E. Fornasiero, and S. Bolognani, "Effect of stator and rotor saturation on sensorless rotor position detection," *IEEE Transactions on Industry Applications*, vol. 49, no. 3, pp. 1333–1342, May 2013.
- [5] J.-H. Jang, S.-K. Sul, J.-I. Ha, K. Ide, and M. Sawamura, "Sensorless drive of surface-mounted permanent-magnet motor by high-frequency signal injection based on magnetic saliency," *IEEE Trans. Industry Applications*, vol. 39, pp. 1031–1039, 2003.
- [6] A. K. Jebai, F. Malrait, P. Martin, and P. Rouchon, "Sensorless position estimation and control of permanent-magnet synchronous motors using a saturation model," *International Journal of Control*, vol. 89, no. 3, pp. 535–549, 2016.
- [7] G. Stumberger, B. Polajzer, B. Stumberger, M. Toman, and D. Dolinar, "Evaluation of experimental methods for determining the magnetically nonlinear characteristics of electromagnetic devices," *IEEE Transactions on Magnetics*, vol. 41, no. 10, pp. 4030–4032, Oct 2005.
- [8] P. Jansen and R. Lorenz, "Transducerless position and velocity estimation in induction and salient AC machines," *IEEE Trans. Industry Applications*, vol. 31, pp. 240–247, 1995.
- [9] A. Jebai, F. Malrait, P. Martin, and P. Rouchon, "Estimation of saturation of permanent-magnet synchronous motors through an energy-based model," in *IEEE International Electric Machines & Drives Conference*, 2011, pp. 1316–1321.
- [10] P. Combes, F. Malrait, P. Martin, and P. Rouchon, "Modeling and identification of synchronous reluctance motors," in *IEEE International Electric Machines & Drives Conference*, 2017.
- [11] A. Jebai, P. Combes, F. Malrait, P. Martin, and P. Rouchon, "Energy-based modeling of electric motors," in *IEEE Conference on Decision and Control*, 2014, pp. 6009–6016.
- [12] P. Combes, A. K. Jebai, F. Malrait, P. Martin, and P. Rouchon, "Energy-based modeling of AC motors," *ArXiv e-prints*, 2016, arXiv:1609.08050 [math.OC].
- [13] J. Melkebeek and J. Willems, "Reciprocity relations for the mutual inductances between orthogonal axis windings in saturated salient-pole machines," *Industry Applications, IEEE Transactions on*, vol. 26, no. 1, pp. 107–114, Jan 1990.
- [14] A. R. Weber and G. Steiner, "An accurate identification and compensation method for nonlinear inverter characteristics for ac motor drives," in *2012 IEEE International Instrumentation and Measurement Technology Conference Proceedings*, May 2012, pp. 821–826.
- [15] P. Combes, A. K. Jebai, F. Malrait, P. Martin, and P. Rouchon, "Adding virtual measurements by signal injection," in *American Control Conference*, 2016, pp. 999–1005.



(a) $i_s^D \mapsto \Phi_s^D(i_s^D, i_s^Q) - \Phi_M$ for $i_s^Q = 0$ A (—), $i_s^Q = -2$ A (—), $i_s^Q = 2$ A (—)



(b) $i_s^Q \mapsto \Phi_s^Q(i_s^D, i_s^Q)$ for $i_s^D = 0$ A (—), $i_s^D = -2$ A (—), $i_s^D = 2$ A (—)

Figure 7. Comparison of current-flux curves obtained with the classical (dashed lines) and proposed method (solid lines).

due to the power inverter, as the injected signal may be fairly large. Besides, the method provides the inductance matrix (as a function of the current or the flux linkage), which is an interesting piece of information by itself, and can also be used to fit a parametric model to the current-flux relations; indeed, it is numerically better to fit the derivatives of a function than the function itself.